Digital Simulation of Counterflow Regenerator Two-dimensional Model by two relatively new Techniques

A. I. Khandwawala† and O. P. Chawla‡

Two relatively new finite-difference explicit methods, Alternating Direction Approximation and the Dufort and Frankel scheme, have been compared for digital simulation of counterflow thermal regenerators. The methods are applied to evaluate the thermal performance of regenerators. The temperature histories in the solid are considered as functions of two space dimensions. The solutions are programmed to include the effect of gas radiation and variable specific heats of gases. Of the two methods compared, the Alternating Direction Approximation is found to be simpler, easy to apply, and self-starting.

NOTATION

A_1, A_2	see equations (14)
A	heat transfer area of channel [m^2]
A_f	flow area of a channel [m^2]
a	semithickness of wall [m]
Bi	Biot number, ha/K
c	specific heat of chequer material [J/kg K]
Fo	Fourier number
h	total heat transfer coefficient [W/m^2 K]
K	thermal conductivity of solid [W/m K]
L	regenerator height [m]
m	number of steps of integration in x-direction
NTU	number of transfer units
n	number of steps of integration in y-direction
P	perimeter of channel [m]
r	number of steps of integration in time
S	specific heat of fluid [J/m^3 K]
T^*	dimensionless matrix temperature, $\dfrac{T - t''_{in}}{t'_{in} - t''_{in}}$
T	matrix temperature [K]
t	fluid temperature [K]
t^*	dimensionless fluid temperature, $\dfrac{t - t''_{in}}{t'_{in} - t''_{in}}$
V	volume flow rate of fluid, at NTP [m^3/s]
W_1, W_2	sides of regenerator channel [m]
X_1 to X_9	see equations (22)
x	distance from channel surface in a direction perpendicular to fluid flow [m]
x^*	dimensionless distance, x/a
Y_1 to Y_9	see equations (13)
y	distance from regenerator entrance in the fluid flow direction [m]
y^*	dimensionless distance, y/L
Z_1 to Z_6	see equations (16)

Greek Symbols

α	thermal diffusivity, $K/\rho c$ [m^2/s]
Λ	reduced length, hA/VS
ρ	density of matrix material [kg/m^3]
ε	regenerator thermal ratio
τ	time [s]
τ_p	heating or cooling period [s]
τ^*	dimensionless time, τ/τ_p
Ω	reduced time, $\alpha\tau_p/a^2$

Subscripts

i	position in x-direction
j	position in y-direction
k	position in time

Superscripts

$'$	refers to heating period
$''$	refers to cooling period

1 INTRODUCTION

The thermal regenerator is used in many chemical and other industries like metal reducing and steel-making plants, glass-making industries, gas turbine plants, etc. The regenerator preheats the combustion air for the furnace, thereby resulting in better combustion and saving in fuel costs. A thermal regenerator consists of chequer work made of refractory bricks or ceramic materials. The waste gases and air, passing alternately through the passages in the matrix structure, exchange heat with the matrix material. Thus the matrix is alternately heated and cooled. A complete cycle comprises a heating period and a cooling period. Starting from an initial uniform matrix temperature distribution, the temperature histories in the matrix and of the gases become periodic after a large number of cycles of operation, and the regenerator is said to have attained cyclic equilibrium.

The prediction of these temperature histories in the matrix and of the gases during the heating and cooling periods of a regenerator operating under cyclic equilibrium is of practical interest. The effects of varying several operating and design parameters, such as channel dimensions, wall thickness, heating and cooling periods, regenerator height, fluid flow rates, etc. can be

† Reader, Mechanical Engineering Dept, Shri GSITS, Indore-452003 India; presently research scholar in Mechanical Engineering Dept, Indian Institute of Technology, New Delhi-110 029
‡ Chief Design Engineer, ITMMEC, Indian Institute of Technology, New Delhi-110 029, India
Received 26 November 1979 and accepted for publication on 1 April 1980

0142/727X/80/0600-0067$02.00

studied without requiring costly experimentation on actual regenerators.

The earlier investigations on regenerators (**1**)–(**4**) have been carried out from a purely mathematical point of view, without taking the actual regenerator parameters into account. Moreover, most of the workers did not consider the heat conduction in the matrix in a direction perpendicular to fluid flow. Instead, they have used a bulk heat transfer coefficient based on mean solid temperature. This simplification, though it may give fairly accurate values of regenerator effectiveness in a few cases (**2**), does not give accurate results for time variation of air and gas exit temperatures or the extreme solid temperatures, but these are available using the methods described in reference (**3**). Willmott (**2**) has solved the problem considering the finite thermal conductivity of the matrix in the direction perpendicular to heat flow. Manrique and Cardenas (**5**) have solved the same problem using the first-order finite difference technique by taking data from actual regenerators. The latter authors have used the heat-transfer coefficient due to Kistner and Schumacher as referred in (**6**), which does not seem to have included the effect of gas radiation. The present work is undertaken to compare two relatively new finite difference explicit methods for regenerator simulation. The methods have been used earlier to solve the problem of one-dimensional transient heat conduction through a slab (**7**), and have been claimed to be simple and unconditionally stable. One of these two methods, the Dufort and Frankel scheme, has earlier been used by the authors (**8**) for regenerator simulation in which the matrix temperature histories have been considered in only one dimension, i.e., parallel to the flow. It has been shown that the computational effort required by the Dufort and Frankel method is nearly half of that required by the Trapezoidal method (**8**), though both the methods are unconditionally stable, and the accuracy of both of these methods is of the order of $(\Delta\tau)^2$. In the present paper the Alternating Direction Approximation method and the Dufort and Frankel scheme are developed for the simulation of the thermal regenerator, considering finite thermal conductivity of the matrix in the direction perpendicular to flow. These two explicit methods have been selected for the purpose because it is well established (**9**) that these methods require considerably less computation time as compared to many other methods like Crank–Nicolson and Mitchel–Pearce used by Willmott (**2**). At the same time, both of these methods have the accuracy of the order of $(\Delta\tau)^2$ at each step of integration, which is comparable to that of the method used by Willmott (**2**). In the estimation of heat transfer coefficients, the effect of gas radiation is also included. For this purpose computer programs are prepared in the form of tables from graphs of emissivities of carbon dioxide and water vapours (**10**). All the necessary correction factors have also been incorporated in the program. The correlation for convective heat transfer has been taken from reference (**11**).

2 MATHEMATICAL MODEL

The mathematical model consists of representing the regenerator by identical flue passages of rectangular cross-section, each of wall thickness $2a$ and perimeter P. The complicated open-basket or pigeon hole-types of flue passages can also be approximated by rectangular flue passages of equivalent hydraulic diameters, beam lengths, and heat transfer areas. Similarly the complicated solid shapes may also be approximated to an equivalent simple wall thickness a. All the assumptions made in the previous paper by Khandwawala and Chawla (**12**) also apply. These are:

(1) Zero thermal conductivity of the matrix in the y-direction, and finite in the x-direction.
(2) Constant heat transfer coefficient during the heating or the cooling period.
(3) Constant fluid flow rates.
(4) Thermal properties of solid matrix invariant with temperature or position.
(5) Uniform fluid temperature at any cross-section.
(6) Within the fluid, heat conduction in the flow direction is negligible.
(7) Effect of fluid mass entrapped in the channel is negligible (see Appendix A).

Since all the channels are identical, the centre plane of the wall thickness is adiabatic. For this reason, in the mathematical analysis, only half the thickness of matrix wall for a single flue passage has to be considered. For both the schemes of solution used for this paper, it is not necessary to write down the diffusion equations of heat conduction within the matrix, since it will not be used here. The first step is to write the difference quotients for all space derivatives, so that, mathematically the problem appears as a system of first order differential equations, with time as independent variable. To do this, the half matrix wall thickness is divided into m by n equal elements, m perpendicular to flow direction and n in the flow direction. The sides of the elements are Δx and Δy, being unity in the third direction. Next, heat balance equations are written for the heat exchange between the surface element and the gas bulk and also for each element of the wall. The resulting differential equations in non-dimensional form (**12**) are as below (Appendix B):

$$\frac{\partial T_1^*}{\partial \tau^*} = \frac{\Omega}{(\Delta x^*)^2}(T_2^* - T_1^*) + \frac{Bi\Omega}{\Delta x^*}(t^* - T_1^*) \tag{1}$$

$$\frac{\partial T_i^*}{\partial \tau^*} = \frac{\Omega}{(\Delta x^*)^2}(T_{i+1}^* - T_i^*) + \frac{\Omega}{(\Delta x^*)^2}(T_{i-1}^* - T_i^*) \qquad i = 2, 3, \ldots, m-1 \tag{2}$$

and

$$\frac{\partial T_m^*}{\partial \tau^*} = \frac{\Omega}{(\Delta x^*)^2}(T_{m-1}^* - T_m^*) \tag{3}$$

An energy balance on the elementary gas volume in the flue section of height Δy gives:

$$\frac{\partial t^*}{\partial y^*} = \Lambda(T_1^* - t^*) \tag{4}$$

In the above eqs (1) to (4), the suffix on T refers to the location of the element in the x-direction.

The conditions of cyclic equilibrium and flow reversal for counterflow regenerator are:

$$T^{*\prime}(x^*, y^*, 1) = T^{*\prime\prime}(x^*, 1 - y^*, 0) \quad (5a)$$

$$T^{*\prime\prime}(x^*, y^*, 1) = T^{*\prime}(x^*, 1 - y^*, 0) \quad (5b)$$

In eqs (5a) and (5b), the third dimension in the nomenclature T^* is the dimensionless time τ^*.

The conditions of constant fluid inlet temperatures can be expressed as:

$$\left.\begin{aligned} t^{*\prime}(0, \tau^{*\prime}) &= 1 \\ t^{*\prime\prime}(0, \tau^{*\prime\prime}) &= 0 \end{aligned}\right\} \quad (6)$$

3 NUMERICAL METHODS

3.1 Alternating Direction Approximation (Appendix C):

The solutions to eqs (1) to (3) using Alternating Direction Approximation are given by the following set of equations, for $j = 1, 2, 3, \ldots, n$:

1. At odd time steps, ($k = 2, 4, 6, \ldots$):

$$T^*_{1,j,k+1} = Y_1 T^*_{1,j,k} + Y_2 t^*_{j,k+1} + Y_3 T^*_{2,j,k} \quad (7)$$

$$T^*_{i,j,k+1} = Y_4 T^*_{i,j,k} + Y_5 (T^*_{i-1,j,k+1} + T^*_{i+1,j,k}) \qquad i = 2, 3, \ldots, m-1 \quad (8)$$

and

$$T^*_{m,j,k+1} = Y_6 T^*_{m,j,k} + Y_5 T^*_{m-1,j,k+1} \quad (9)$$

2. At even time steps, ($k = 1, 3, 5, \ldots$):

$$T^*_{m,j,k+1} = Y_7 T^*_{m,j,k} + A_1 T^*_{m-1,j,k} \quad (10)$$

$$T^*_{i,j,k+1} = Y_4 T^*_{i,j,k} + Y_5 (T^*_{i-1,j,k} + T^*_{i+1,j,k+1}) \qquad i = m-1, m-2, \ldots, 3, 2 \quad (11)$$

and

$$T^*_{1,j,k+1} = Y_8 T^*_{1,j,k} + Y_9 t^*_{j,k} + Y_5 T^*_{2,j,k+1} \quad (12)$$

In the above equations,

$$\left.\begin{aligned} Y_1 &= \frac{1 - A_1}{1 + A_2} & Y_2 &= \frac{A_2}{1 + A_2} \\ Y_3 &= \frac{A_1}{1 + A_2} & Y_4 &= \frac{1 - A_1}{1 + A_1} \\ Y_5 &= \frac{A_1}{1 + A_1} & Y_6 &= \frac{1}{1 + A_1} \\ Y_7 &= 1 - A_1 & Y_8 &= \frac{1 - A_2}{1 + A_1} \end{aligned}\right\} \quad (13)$$

and

$$Y_9 = \frac{A_2}{1 + A_1}$$

where

$$A_1 = \frac{\Delta\tau^*\Omega}{(\Delta x^*)^2} \quad \text{and} \quad A_2 = \frac{\Delta\tau^*\Omega Bi}{\Delta x^*} \quad (14)$$

For the integration of eq (4), the trapezoidal formula may be used, giving

$$t^*_{j,k+1} = Z_1 t^*_{j-1,k+1} + Z_2 (T^*_{1,j,k+1} + T^*_{1,j-1,k+1}) \qquad j = 2, 3, \ldots, n \quad (15)$$

where

$$Z_1 = (1 - 0{\cdot}5\Lambda\Delta y^*)/(1 + 0{\cdot}5\Lambda\Delta y^*)$$

$$Z_2 = \frac{0{\cdot}5\Lambda\Delta y^*}{1 + 0{\cdot}5\Lambda\Delta y^*} \quad (16a)$$

The solution (15) cannot be used to calculate the gas temperatures at odd time steps, as it requires prior knowledge of matrix temperatures, $T^*_{1,j,k+1}$, at the same time step. For this purpose, eqs (7) to (12) and (15) are combined to give:

$$t^*_{j,k+1} = Z_3 t^*_{j-1,k+1} + Z_4 T^*_{1,j-1,k+1} + Z_5 T^*_{1,j,k} + Z_6 T^*_{2,j,k} \quad (17)$$

where

$$\left.\begin{aligned} Z_3 &= \frac{Z_1}{1 - Z_2 Y_2} & Z_4 &= \frac{Z_2}{1 - Z_2 Y_2} \\ Z_5 &= \frac{Z_2 Y_1}{1 - Z_2 Y_2} & Z_6 &= \frac{Z_2 Y_3}{1 - Z_2 Y_2} \end{aligned}\right\} \quad (16b)$$

The scheme of solution by this method is shown in flow chart, Fig. 1(a).

3.2 Dufort and Frankel Scheme (Appendix C).

The solutions of eqs (1) to (4) using the Dufort and Frankel scheme are given by the next set of equations (18) to (20) for $j = 1, 2, \ldots, n$, $k = 2, 3, \ldots, r-1$ and by eq. (21).

$$T^*_{1,j,k+1} = X_1 T^*_{1,j,k-1} + X_2 T^*_{2,j,k} + X_3 t^*_{j,k} \quad (18)$$

$$T^*_{i,j,k+1} = X_4 T^*_{i,j,k-1} + X_5 (T^*_{i+1,j,k} + T^*_{i-1,j,k}) \qquad i = 2, 3, \ldots, m-1 \quad (19)$$

$$T^*_{m,j,k+1} = X_6 T^*_{m,j,k-1} + X_7 T^*_{m-1,j,k} \quad (20)$$

$$t^*_{j+1,k} = X_8 t^*_{j-1,k} + X_9 T^*_{1,j,k} \qquad k = 1, 2, \ldots, r;\ j = 2, 3, \ldots, n-1 \quad (21)$$

where

$$\left.\begin{aligned} X_1 &= \frac{1 - A_1 - A_2}{1 + A_1 + A_2} & X_2 &= \frac{2A_1}{1 + A_1 + A_2} \\ X_3 &= \frac{2A_2}{1 + A_1 + A_2} & X_4 &= \frac{1 - 2A_1}{1 + 2A_1} \\ X_5 &= \frac{2A_1}{1 + 2A_1} & X_6 &= \frac{1 - A_1}{1 + A_1} \\ X_7 &= \frac{2A_1}{1 + A_1} & X_8 &= \frac{1 - \Delta y^*\Lambda}{1 + \Delta y^*\Lambda} \end{aligned}\right\} \quad (22)$$

$$X_9 = \frac{2\Delta y^*\Lambda}{1 + \Delta y^*\Lambda}$$

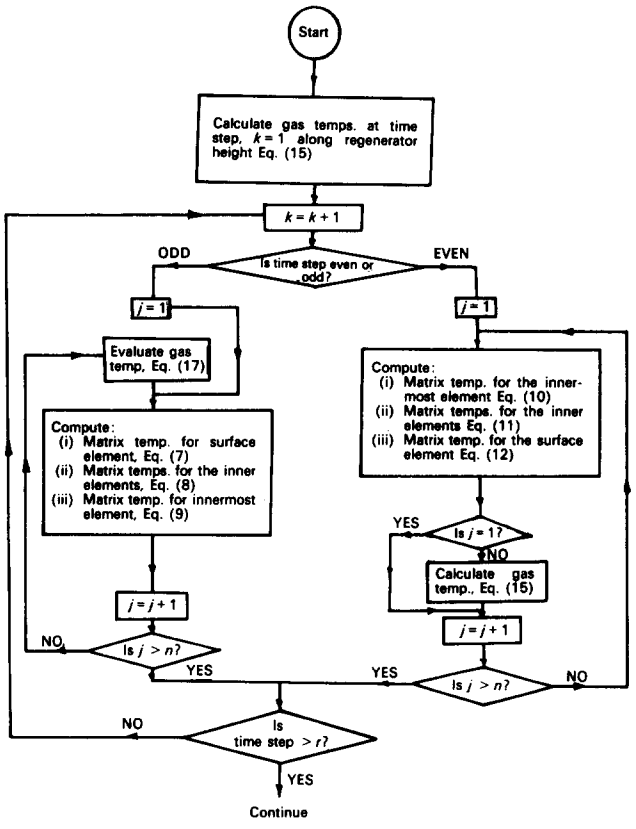

Fig. 1a. Flow chart for Alternating Direction Approximation method

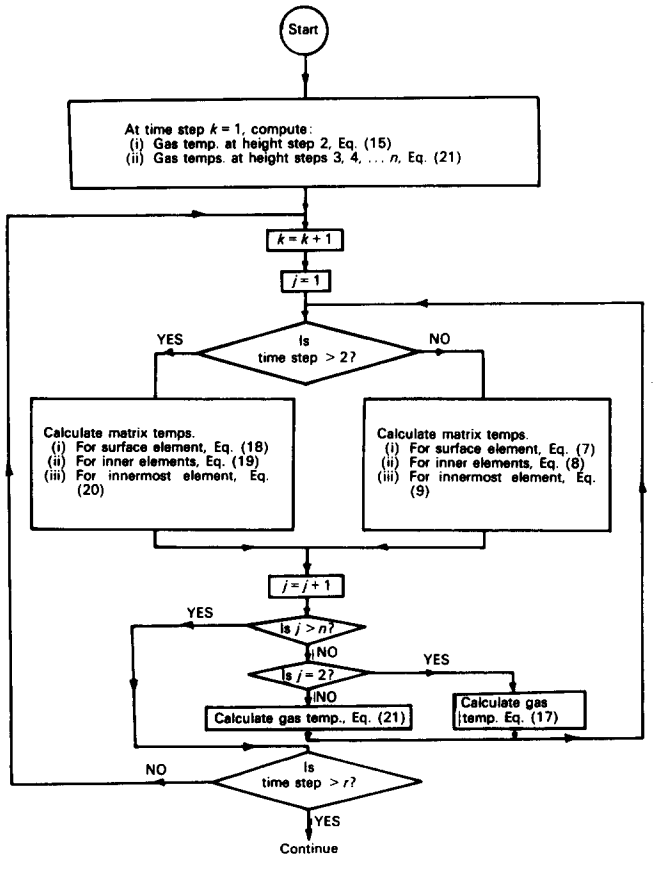

Fig. 1b. Flow chart for Dufort and Frankel scheme

The solutions (18) to (21) are multi-step, i.e., eqs (18) to (20) cannot be used for $k = 1$ (time step 2), and eq. (21) cannot be used at height step j equal to 2. Hence other methods have to be used for starting the solution. In the present work eqs (7) to (9), (15), and (17) are used for starting the solution. The scheme is shown in the flow chart, Fig. 1b.

The complete step-by-step simulation procedure for either scheme is shown in the flow chart Fig. 2. To start with, an arbitrary but well chosen temperature distribution is assumed at the beginning of the heating period. Values of air and gas specific heats, and the overall heat transfer coefficients for both the periods are also suitably assumed. The matrix and fluid temperatures during heating and cooling periods for the first iteration are calculated following the scheme shown in Figs. 1 and 2. At the end of the first iteration, the time average exit temperatures of the air and the hot gases, $\bar{t}''_{exit}$ and $\bar{t}'_{exit}$, are calculated. The fluid specific heats and

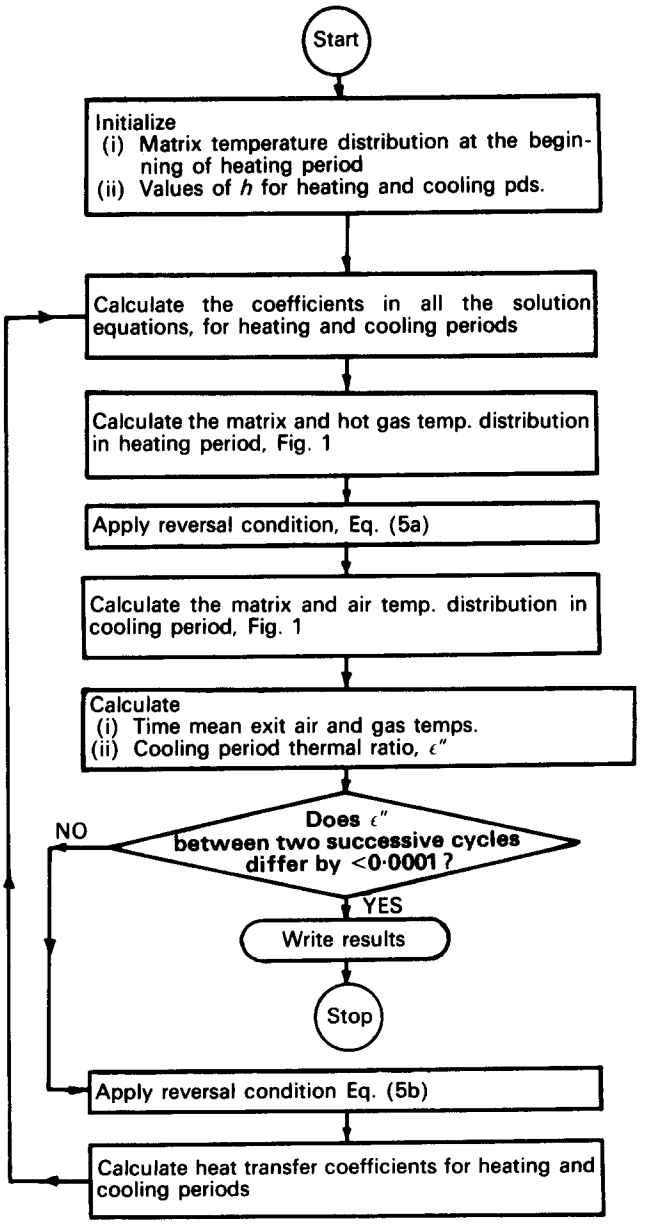

Fig. 2. Regenerator simulation

the heat transfer coefficients required for calculating the coefficients in all the equations in the next iteration are then based on t'_{mean} for the heating period and t''_{mean} for the cooling period, where,

$$t'_{mean} = \tfrac{1}{2}(\bar{t}'_{exit} + t'_{in})$$

and

$$t''_{mean} = \tfrac{1}{2}(\bar{t}''_{exit} + t''_{in})$$

The surface temperature for both the periods is assumed as the arithmetic mean of t'_{mean} and t''_{mean}.

The iteration is terminated when both the following criteria are satisfied:

(i) the cooling period thermal ratios, ε'', between two successive cycles differ by less than 0·0001

(ii) the 'improved convergence criterion'

$$\left| \frac{(\varepsilon''_n - \varepsilon''_{n-1})^2}{\varepsilon''_n - 2\varepsilon''_{n-1} + \varepsilon''_{n-2}} \right| < 0{\cdot}0001$$

is satisfied.

Here ε''_n is the cooling period thermal ratio in the nth cycle of iteration and ε'' is defined as

$$\varepsilon'' = \frac{\bar{t}''_{exit} - t''_{in}}{t'_{in} - t''_{in}}$$

The improved convergence criterion has been proposed by Willmott and Kulakowski (**13**) to minimize the danger of mistaking slow convergence for cyclic equilibrium. This improved criterion has not been shown in the flow chart, Fig. 2, although it was incorporated in the computer programs run for the present paper. As a further check on convergence, heat balances for some of the computed examples are presented in Appendix D.

4 RESULTS AND DISCUSSION

To demonstrate the usefulness of the two methods, and to compare them, a regenerator with the following data has been considered:

Hot gas inlet temperature: 1723 K
Air inlet temperature: 323 K
Thermal conductivity of solid: 1·581 W/m K
Thermal diffusivity of solid: 4×10^{-7} m^2/s
Emissivity of surface: 0·8
Heating and cooling periods, each: 1200 s
Ratio of gas to air flow: 1·045

Gas composition, percentage by volume (pressure 1 atm):

$CO_2 = 12{\cdot}33$
$H_2O = 11{\cdot}36$
$N_2 = 74.51$
$O_2 = 1{\cdot}80$

The channel dimensions are:

$W_1 = 0{\cdot}1524$ m
$W_2 = 0{\cdot}2286$ m
$a = 0{\cdot}0381$ m

Regenerator heights varying from 2·5 m up to 9 m are considered for this example, keeping the flow rate of air fixed at 0·01527 m^3/s. Next for the regenerator height of 5·5 m, the flow rates are changed to 90 per cent, 120 per cent, and 140 per cent of the above value. Thus it has been possible to cover a wide range of regenerator thermal ratios.

The programs were run on ROBOTRON ES1040 computer, taking $m = 6$, $n = 12$, and $r = 21$, for both the methods. The program size and computer core required for both the methods were more or less the same. The thermal ratios calculated by the two methods for different regenerator heights and flow rates are compared in Table 1a.

In Table 1b the air preheat temperatures at the beginning and at the end of the cooling period are listed. Table 1b also depicts the maximum matrix temperature (which occurs at the surface at inlet in the end of the heating period) and the minimum matrix temperature (which occurs at the surface at inlet in the end of the cooling period).

From Table 1a it is evident that the cooling period thermal ratios calculated by Alternating Direction approximation agree within 0·1 per cent with the corresponding thermal ratios calculated by the Dufort and Frankel scheme. The heating period thermal ratios are close up to about 1 per cent.

From Table 1b it is observed that the preheat temperatures and the matrix extreme temperatures calculated by both the methods are in very close agreement.

The number of cycles to equilibrium by both the methods were exactly the same in each case. The computer time required by Alternating Direction Approximation for the data of Sr. No. 1, Table 1, was 31 seconds, whereas by the Dufort and Frankel scheme, it was 33 seconds. For the data of Sr. No. 4 Table 1, the respective times by both the methods were 39 seconds and 42 seconds. The computation time for all other examples worked out by both the methods were in similar proportion.

In another set of examples, the channel dimensions are changed to $W_1 = 0{\cdot}165$ m, $W_2 = 0{\cdot}171$ m and $a = 0{\cdot}0317$ m, keeping all other data the same. Again for varying flow rates and regenerator heights, the results are displayed in Tables 2a and 2b. Here again a close agreement between the results is found by both the methods.

These results are also in agreement with the very limited experimental data available from actual regenerators operating in industry.

Both the methods used in the present work are found to be stable for any step size. Results from a non-linear example worked out by the authors suggest that these methods are stable in non-linear cases as well. Any one of the two methods can be used for predicting the thermal performance of a regenerator using a two-dimensional model. But it can be seen that in the Alternating Direction Method fewer coefficients are required to be calculated. So the amount of computation in this method is slightly less than in the other method. For the same reason, this method is expected to need, relatively, still less computer time for the non-linear problem. This is in relation to the fact that in the non-linear problem the coefficients are to be calculated at each step of integration.

Table 1: Comparison of two methods for $W_1 = 0{\cdot}1524$ m, $W_2 = 0{\cdot}2286$ m, and $a = 0{\cdot}0381$ m

(a) Thermal ratios

Sr. No.	V'' m³/s	L m	Alternating direction		Dufort and Frankel	
			ε'	ε''	ε'	ε''
1	0·01527	2·5	0·2476	0·3089	0·2442	0·3085
2	0·01527	3·5	0·3167	0·3926	0·3132	0·3923
3	0·01527	4·5	0·3734	0·4604	0·3698	0·4603
4	0·01527	5·5	0·4233	0·5154	0·4192	0·5156
5	0·01527	7·5	0·4978	0·6012	0·4926	0·6023
6	0·01527	9·0	0·5512	0·6473	0·5445	0·6492
7	0·01382	5·5	0·4311	0·5250	0·4269	0·5254
8	0·01833	5·5	0·4078	0·4994	0·4036	0·4994
9	0·02138	5·5	0·4039	0·4850	0·3987	0·4851

(b) Air and extreme solid temperatures (dimensionless)

Sr. No.	Alternating direction				Dufort and Frankel			
	Preheat temperature		Solid temperature		Preheat temperature		Solid temperature	
	Beginning of period	End of period	Max.	Min.	Beginning of period	End of period	Max.	Min.
1	0·3265	0·2998	0·9178	0·5976	0·3275	0·2998	0·9200	0·5976
2	0·4134	0·3818	0·9256	0·5394	0·4148	0·3820	0·9275	0·5395
3	0·4829	0·4487	0·9321	0·4922	0·4846	0·4491	0·9339	0·4924
4	0·5386	0·5034	0·9375	0·4498	0·5408	0·5041	0·9392	0·4506
5	0·6240	0·5892	0·9741	0·3895	0·6270	0·5908	0·9487	0·3914
6	0·6691	0·6358	0·9526	0·3404	0·6729	0·6382	0·9542	0·3433
7	0·5465	0·5138	0·9414	0·4506	0·5487	0·5147	0·9430	0·4515
8	0·5258	0·4858	0·9315	0·4507	0·5279	0·4863	0·9334	0·4513
9	0·5145	0·4699	0·9281	0·4324	0·5170	0·4706	0·9302	0·4322

Table 2: Comparison of two methods for $W_1 = 0{\cdot}165$ m, $W_2 = 0{\cdot}171$ m, and $a = 0{\cdot}0317$ m

(a) Thermal ratios

Sr. No.	V'' m³/s	L m	Alternating direction		Dufort and Frankel	
			ε'	ε''	ε'	ε''
1	0·01142	3·5	0·3451	0·4270	0·3402	0·4263
2	0·01142	5·5	0·4520	0·5521	0·4467	0·5520
3	0·01142	7·5	0·5223	0·6369	0·5156	0·6379
4	0·01142	9·0	0·5565	0·6850	0·5488	0·6865
5	0·01028	5·5	0·4367	0·5605	0·4574	0·5610
6	0·01317	5·5	0·4386	0·5354	0·4327	0·5351
7	0·01599	5·5	0·4292	0·5209	0·4228	0·5204

(b) Air and extreme solid temperatures (dimensionless)

Sr. No.	Alternating direction				Dufort and Frankel			
	Preheat temperature		Solid temperature		Preheat temperature		Solid temperature	
	Beginning of period	End of period	Max.	Min.	Beginning of period	End of period	Max.	Min.
1	0·4481	0·4160	0·9227	0·5173	0·4500	0·4161	0·9303	0·5170
2	0·5747	0·5403	0·9411	0·4285	0·5774	0·5411	0·9433	0·4291
3	0·6583	0·6256	0·9492	0·3708	0·6620	0·6274	0·9513	0·3727
4	0·7049	0·6745	0·9546	0·3448	0·7090	0·6768	0·9566	0·3475
5	0·5813	0·5495	0·9452	0·4250	0·5845	0·5508	0·9463	0·4259
6	0·5612	0·5220	0·9336	0·4261	0·5462	0·5227	0·9363	0·4267
7	0·5497	0·5060	0·9281	0·4198	0·5529	0·5066	0·9310	0·4200

5 CONCLUSION

The results obtained by the two methods are quite close, and compare favourably with very limited data available from experiments on actual regenerators. The effects of varying regenerator parameters obtained in these investigations are similar to those obtained by Manrique and Cardenas (**5**). These methods are simpler to apply and can be used with any type of boundary conditions, and variable properties of solid and fluids. The Alternating Direction Approximation is the simpler of the two methods, as it is self-starting, and it requires relatively less computer time.

REFERENCES

(1) CHASE, C. A., Jr., GIDASPOW, D., and PECK, R. E. 'A regenerator prediction of Nusselt numbers', *Int. J. Heat Mass Transfer*, 1969, **12**, 727–736.

(2) WILLMOTT, A. J. 'The regenerative heat exchanger computer representation', *Int. J. Heat Mass Transfer*, 1969, **12**, 997–1014.

(3) EDWARDS, J. V., EVANS, R., and PROBERT, S. D. 'Computation of transient temperatures in regenerators', *Int. J. Heat Mass Transfer*, 1971, **14**, 1175–1202.

(4) WILLMOTT, A. J. and THOMAS, R. J. 'Analysis of the long contraflow regenerative heat exchanger', *J. Inst. Math. Applic*, 1974, **14**, 267–280.

(5) MANRIQUE, A. J. and CARDENAS, R. S. 'Digital simulation of a regenerator', *Fifth Int. Heat Transfer Conf.* V Tokyo 1974, 190–194.

(6) SCHACK, A. *Industrial Heat Transfer*, 1965 (John Wiley).

(7) LARKIN, B. K. 'Some finite difference methods for problems in transient heat flow', *Chem. Engng. Prog. Symp. Series*, 1965, **61**, No. 59, 1–11.

(8) KHANDWAWALA, A. I. and CHAWLA, O. P. 'Computer simulation of thermal performance of regenerators by different methods', *Reg. J. Energy Heat Mass Transfer*, 1978, **1**, 21–26.

(9) JAIN, M. K. *Numerical solution of Differential equations*, 1979 (Wiley Eastern, New Delhi).

(10) HOTTEL, H. C. and SAROFIN, A. F. *Radiative Heat Transfer*, 1967 (McGraw Hill, New York).

(11) RAZELOS, P. and PASCHKIS, V. 'The thermal design of blast furnace stoves regenerators', *Iron Steel Engr*, Aug. 1968, 81–116.

(12) KHANDWAWALA, A. I. and CHAWLA, O. P. 'Digital simulation of two-dimensional regenerator model', *Engineer, IME* (India), to be published in June–Dec., 1979 issue.

(13) WILLMOTT, A. J. and KULAKOWSKI, B. 'Numerical acceleration of thermal regenerator simulation', *Int. J. Numr. Methods Engr.* 1977, **11**, 533–551.

APPENDIX A

Effect of Neglecting the Heat Capacity of Fluid Within Regenerator Channels

The equation of heat exchange between the wall surface element and the gas bulk is:

$$hP\Delta y(T_1 - t) = VS\frac{\partial t}{\partial y}\Delta y + A_f \Delta y S\frac{\partial t}{\partial \tau}$$

or

$$\frac{hP}{S}(T_1 - t) = V\frac{\partial t}{\partial y} + A_f\frac{\partial t}{\partial \tau} \qquad (1)$$

In the various examples worked out by the authors, the maximum value of $\partial t/\partial \tau$ occurred at the gas exit for $\tau = 0$, whereas the value of $\partial t/\partial y$ was almost constant. For the data of Table 1, Sr. No. 1 of this paper, the maximum value of $\partial t/\partial \tau$ was 0·1917 K/s. At this point, the value of $\partial t/\partial y$ was 165·3 K/m. The ratio of second term to first term on the right-hand side of eq. (1) is therefore:

$$R = \frac{0{\cdot}2286 \times 0{\cdot}1524 \times 0{\cdot}1917}{0{\cdot}01596 \times 165{\cdot}3} = 2{\cdot}53 \times 10^{-3}$$

The values of R of this magnitude occurred only at three or four grid points. At the other grid points the values of R worked out to be still less, of the order of 10^{-5} and still lower. Hence it was justifiable to neglect the second term on the right-hand side of eq. (1) in comparison with the first term.

APPENDIX B

Derivation of Heat Balance Equations (1) to (4)

Referring to Fig. A.1, the heat balance equations for the matrix elements, at any height step j, are written as follows:

(a) For the surface element, $i = 1$,

$$\rho c\Delta x\Delta y\frac{\partial T_1}{\partial \tau} = K\frac{\Delta y}{\Delta x}(T_2 - T_1) + h(t - T_1)\Delta y$$

or

$$\frac{\partial T_1}{\partial \tau} = \frac{K}{\rho c(\Delta x)^2}(T_2 - T_1) + \frac{h}{\rho c\Delta x}(t - T_1) \qquad (i)$$

Here the suffix on T refers to the position of the element in the x-direction.

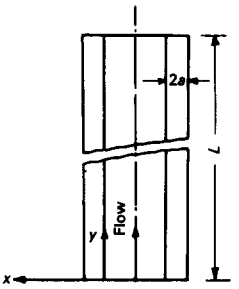

(a)

Fig. A.1(a). Regenerator channel

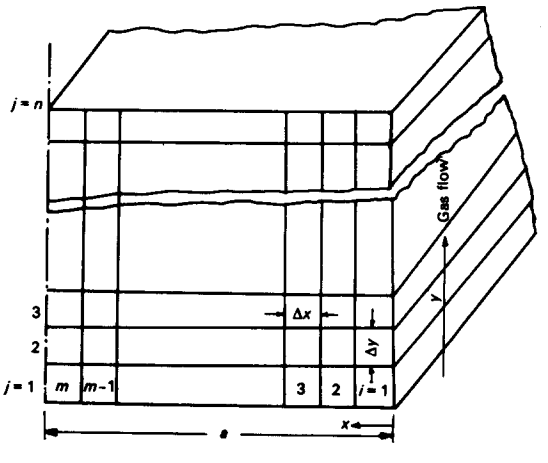

(b)

Fig. A.1(b). Semithickness of wall (enlarged) divided into elements for writing heat balance equations

(b) For the inner elements, $i = 2$ to $i = m - 1$,

$$\rho c \Delta x \Delta y \frac{\partial T_i}{\partial \tau} = \frac{K \Delta y}{\Delta x}(T_{i+1} - T_i) + \frac{K \Delta y}{\Delta x}(T_{i-1} - T_i)$$

or

$$\frac{\partial T_i}{\partial \tau} = \frac{K}{\rho c (\Delta x)^2}(T_{i+1} - T_i) + \frac{K}{\rho c (\Delta x)^2}(T_{i-1} - T_i) \qquad \text{(ii)}$$

(c) For the innermost element, having one surface adiabatic, $i = m$

$$\rho c \Delta x \Delta y \frac{\partial T_m}{\partial \tau} = \frac{K \Delta y}{\Delta x}(T_{m-1} - T_m)$$

or

$$\frac{\partial T_m}{\partial \tau} = \frac{K}{\rho c (\Delta x)^2}(T_{m-1} - T_m) \qquad \text{(iii)}$$

The heat exchange between the surface element and the gas bulk in the channel cross-section at height j balances to†

$$hP\Delta y(T_1 - t) = VS\frac{\partial t}{\partial y}\Delta y + A_f \Delta y S \frac{\partial t}{\partial \tau}$$

The second term in the above equation represents the rate of increase in the heat content of the hold up fluid. It is ignored, being small in comparison with the first term (Appendix A). Hence this equation reduces to

$$\frac{\partial t}{\partial y} = \frac{hP}{VS}(T_1 - t) \qquad \text{(iv)}$$

The equations (i) to (iv) are transformed to non-dimensional form by making the following substitutions:

$$x^* = x/a$$

$$y^* = y/L$$

$$T^* = \frac{T - t''_{in}}{t'_{in} - t''_{in}}$$

$$t^* = \frac{t - t''_{in}}{t'_{in} - t''_{in}}$$

$$\alpha = \frac{K}{\rho c}$$

$$\tau^* = \tau/\tau_p$$

$$Bi = \frac{ha}{K}$$

$$\Omega = \frac{\alpha \tau_p}{a^2}$$

$$\Lambda = \frac{hA}{VS}$$

† In this equation the specific heat of the fluid is taken on volumetric basis at NTP conditions. As the air-handling equipments are usually rated on volume basis rather than on mass basis, the practice in industry is to rate the regenerators and furnaces on volume flow rates. Therefore the authors have thought it appropriate to use the volumetric specific heat of gases.

In the above transformation, the reduced time Ω is equivalent to a Fourier number Fo, and the reduced length Λ may be interpreted as NTU.

The resulting transformed equations are:

$$\frac{\partial T_1}{\partial \tau^*} = \frac{\Omega}{(\Delta x^*)^2}(T_2^* - T_1^*) + \frac{\Omega Bi}{\Delta x^*}(t^* - T_1^*) \qquad (1)$$

$$\frac{\partial T_i^*}{\partial \tau^*} = \frac{\Omega}{(\Delta x^*)^2}(T_{i+1}^* - T_i^*) + \frac{\Omega}{(\Delta x^*)^2}(T_{i-1}^* - T_i^*)$$

$$i = 2, 3, \ldots m - 1 \qquad (2)$$

$$\frac{\partial T_m^*}{\partial \tau^*} = \frac{\Omega}{(\Delta x^*)^2}(T_{m-1}^* - T_m^*) \qquad (3)$$

and

$$\frac{\partial t^*}{\partial y^*} = \Lambda(T_1^* - t^*) \qquad (4)$$

APPENDIX C

Two Integrating Schemes

In a set of m elements, the heat-balance equation for the element i, exchanging heat with p elements, will be of the form:

$$\frac{dT_i}{d\tau} = \sum_{q=1}^{p} R_{q,i}(T_q - T_i) \qquad i = 1, 2, \ldots, m \qquad (1)$$

where $R_{q,i}$ is the thermal conductance between the elements i and q. It may be noted that $R_{i,i} = 0$.

The Alternating Direction Approximation to eq. (1) is given by the following two sets of formulae (7):

$$T_{i,k+1} = \frac{T_{i,k} + \Delta\tau \sum_{q=1}^{i} R_{q,i} T_{q,k+1}}{1 + \Delta\tau \sum_{q=1}^{i} R_{q,i}} + \frac{\Delta\tau \sum_{q=i+1}^{p} R_{q,i}(T_{q,k} - T_{i,k})}{1 + \Delta\tau \sum_{q=1}^{i} R_{q,i}}$$

at odd times, i increasing

and

$$T_{i,k+2} = \frac{T_{i,k+1} + \Delta\tau \sum_{q=1}^{i} R_{q,i}(T_{q,k+1} - T_{i,k+1})}{1 + \Delta\tau \sum_{q=i+1}^{p} R_{q,i}} + \frac{\Delta\tau \sum_{q=i+1}^{p} R_{q,i} T_{q,k+1}}{1 + \Delta\tau \sum_{q=i+1}^{p} R_{q,i}}$$

at even times, i decreasing.

The corresponding Dufort and Frankel Approximation of eq. (1) is given by the following three-level formula (7):

$$T_{i,k+1} = \frac{T_{i,k-1} + \Delta\tau \sum_{q=1}^{p} R_{q,i}(2T_{q,k} - T_{i,k-1})}{1 + \Delta\tau \sum_{q=1}^{p} R_{q,i}}$$

In the above equations, the second suffix on T, that is, k, represents the stage of integration.

APPENDIX D

Heat Balance Checks for Convergence

As a further check on cyclic equilibrium, heat balances have been made for some examples. As the heating period and the cooling period are equal in each example quoted in this paper, the rate of heat loss by waste gases in passing through the regenerator in the heating period should be equal to the rate of heat gain by air in passing through the regenerator in the cooling period. These are tabulated below:

Example referred	Rate of heat loss by waste gases, kW	Rate of heat gain by air, kW
2 in Table 1	12·3692	12·4215
3 in Table 1	14·521	14·558
4 in Table 1	16·387	16·289
5 in Table 1	19·156	19·029
8 in Table 1	18·977	18·941
1 in Table 2	10·016	10·092
2 in Table 2	13·041	13·041
3 in Table 2	14·982	15·091
6 in Table 2	15·205	15·181